



ELSEVIER

Colloids and Surfaces

A: Physicochemical and Engineering Aspects 000 (1998) 000-000

COLLOIDS
AND
SURFACES

A

Characterization of aggregation phenomena by means of acoustic and electroacoustic spectroscopy

Andrei S. Dukhin *, Philip J. Goetz

Dispersion Technology Inc., 3 Hillside Avenue, Mount Kisco, NY 10549, USA

Received 19 September 1997; received in revised form 20 March 1998; accepted 24 April 1998

Abstract

Aggregation phenomena change the particle-size distribution, replacing small particles with larger aggregates. Measuring this evolution of particle size is an apparent way to characterize aggregation phenomena. It is often desirable to perform this measurement in an intact, concentrated, dispersed system. Until recently, this kind of measurement was impossible, but the situation has improved dramatically with the availability of ultrasound-based spectroscopy. An ultrasound pulse interacts with dispersed particles while propagating through the dispersed system, thereby attenuating. An acoustic spectrometer measures this attenuation for a set of frequencies and calculates the corresponding particle size. An ultrasound pulse also disturbs the particle double layer. As a result, the particles generate an electric current, the so-called colloid vibration current (CVI). An electroacoustic spectrometer measures this current and calculates the ζ potential. We have suggested in our previous papers that combined acoustic and electroacoustic spectroscopy provides the most reliable and complete characterization of concentrated dispersed systems. We show in this paper that this technique is able to determine not only the isoelectric point but also a range of pH where system is not stable. It is found that the system loses stability when the ζ potential becomes less than 30 mV. We prove that a lognormal distribution is not adequate for characterizing unstable systems compared with the performance achieved with a bimodal distribution. © 1998 Elsevier Science B.V.

Keywords: Aggregation phenomena; Acoustic and electroacoustic spectroscopy; Particle-size distribution; Zeta potential

1. Introduction

Acoustic and electroacoustic spectroscopy are developing rapidly as an alternative to light-scattering methods. The ability to characterize concentrated disperse systems provides much of the impetus for these developments. Both techniques are based on a well established scientific background [1-19]. In both methods, the interaction of sound with the dispersed particles provides

useful information. However, the set of measured parameters is different. In acoustic spectroscopy we measure the attenuation and/or sound speed [3-5] whereas for electroacoustic spectroscopy it is either the colloid vibration potential/current (CVP/CVI) [6] or the electrosonic amplitude (ESA) [8,9].

Electroacoustic spectra depend on both particle-size distribution (PSD) and ζ potential, which makes this type of spectroscopy very attractive for providing complex characterization of both these parameters. However, there are several disadvantages to this simple approach. We have analyzed 70

* Corresponding author. Tel.: +1 914 2414791; Fax: +1 914 2414842.

71 and listed these problems in our previous paper
72 [10]. In order to eliminate these limitations we
73 have suggested the combination of electroacoustics
74 with acoustics [10]. This new approach requires
75 more sophisticated hardware. Nevertheless, we
76 believe that it is worthwhile because the reliability
77 of the data improves significantly.

78 Acoustic spectroscopy based on the attenuation
79 measurement does not require any assumptions
80 about electroacoustic properties. As a result, the
81 PSD obtained with acoustic spectroscopy is more
82 reliable than that extracted from the spectra. This
83 means that acoustic spectroscopy is more prefera-
84 ble for the characterization of particle-size distribu-
85 tion. The more reliable PSD coming from acoustic
86 spectroscopy can then be used in interpretation of
87 the electroacoustic spectra. As a result, the
88 improvement in the reliability of PSD determina-
89 tion leads to more reliable ζ -potential data.

90 In this paper, we characterize the accuracy and
91 precision of acoustics and electroacoustics by using
92 stable, well-defined, concentrated dispersed sys-
93 tems. It is shown that this combined acoustic
94 spectroscopy is suitable for characterizing unstable
95 dispersed systems as well. In order to do this, a
96 titration with a concentrated dispersed system has
97 been performed. The change in both measured
98 parameters (attenuation spectra and CVI) reflects
99 changes in the particle-size distribution and ζ
100 potential. Comparison of these two parameters
101 allows us to determine the value of ζ and range of
102 pH at which the system loses stability.

103 Calculation of the PSD from acoustic attenua-
104 tion spectra requires an assumption concerning the
105 shape of the distribution. A lognormal distribution
106 is the most widely used model. Here, we compare
107 the performance of lognormal PSD and bimodal
108 PSD by means of error analysis.

109 2. Measuring technique

110 A combined acoustic and electroacoustic spec-
111 trometer (DT-1200) developed by Dispersion
112 Technology Inc. was used. This instrument has
113 two separate sensors for measuring acoustic and
114 electroacoustic signals separately. Both sensors use
115 a pulse technique.

The acoustic sensor has two piezo crystal trans- 116
ducers. The gap between transmitter and receiver 117
is variable in steps. In default it changes from 118
0.15 mm up to 20 mm in 21 steps. The basic 119
frequency of the pulse changes in steps as well. In 120
default it changes from 3 to 100 MHz in 18 steps. 121
The number of pulses collected for each gap and 122
each frequency is automatically adjustable in order 123
to reach the target signal-to-noise ratio. 124

The acoustic sensor also measures the speed of 125
sound at one chosen frequency by using the time 126
of arrival of the pulse at the receiver. The instru- 127
ment automatically adjusts pulse sampling depend- 128
ing on the value of the speed of sound. This is 129
necessary for eliminating possible artefacts like 130
excess attenuation at low frequencies. 131

The electroacoustic sensor measures the magni- 132
tude and phase of the colloid vibration current at 133
2 MHz. It has a piezo crystal sound transmitter 134
and a specially designed electric antenna. The 135
distance between the transmitter and antenna is 136
5 mm. There is provision for automatic correction 137
for the speed of sound and attenuation measured 138
with the acoustic sensor. 139

All experimental data are stored in an Access 140
database. A special analysis program calculates 141
PSDs from attenuation spectra and ζ potentials 142
from the CVI. This program tests lognormal, 143
bimodal and modified lognormal [20] particle-size 144
distributions and uses an error analysis to search 145
for the best PSD. The goal of the optimization 146
procedure is to minimize the error of the theoretical 147
fit of the experimental attenuation spectra. 148

The analysis program takes into account a PSD 149
correction when calculating the ζ potential. It uses 150
either the PSD calculated from the attenuation 151
spectra or a PSD known a priori. It makes also 152
correction for attenuation of the sound pulse 153
resulting from backflow caused by moving dis- 154
persed particles. An additional correction is made 155
for the volume fraction effect, which is required in 156
concentrated dispersed systems. 157

The instrument also has a special prediction 158
program. This is an educational tool that gives the 159
opportunity to calculate attenuation and CVI 160
spectra for any system specified by the user. This 161
program is suitable also for a manual search of 162
the best PSD for the given experimental attenua- 163

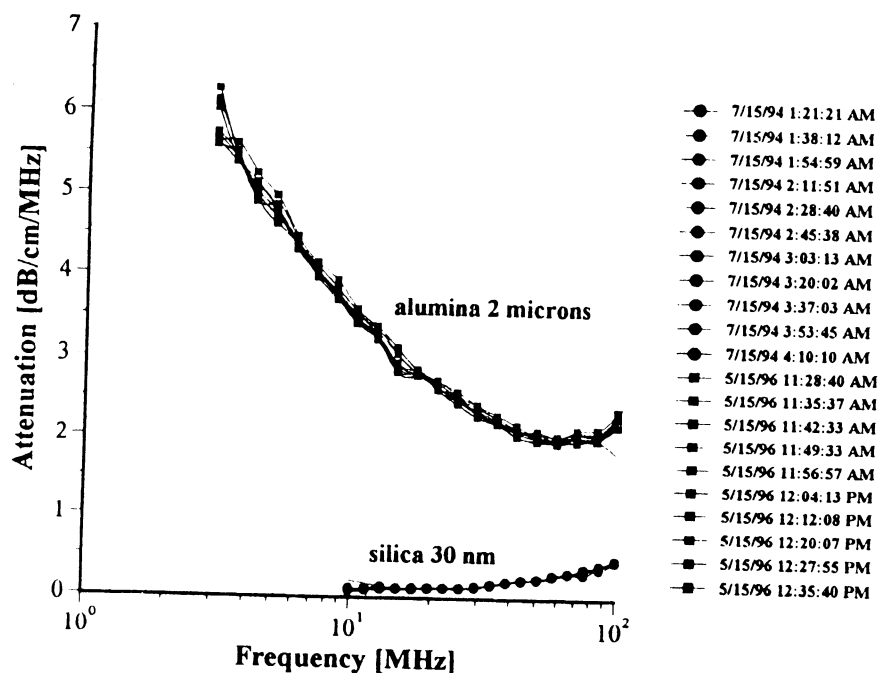


Fig. 1. Attenuation of the multiple measurements with alumina Sumitomo AA-2 and silica Ludox.

8
12

164 tion spectra. It helps to overcome the problem of
165 a local minimum which might be an obstacle for
166 the automatic optimization program.

167 The total volume of sample required is about
168 100 ml. A special magnetic stirrer prevents sedi-
169 mentation and ensures mixing of the chemicals
170 during titration. The instrument is equipped with
171 two burettes and appropriate software for auto-
172 matic titration. It also has conductivity and tem-
173 perature probes.

174 Measurement of one attenuation spectrum with
175 the default set-up takes about 5 min. The user can
176 speed up the measurements by changing the set-
177 up parameters. One CVI measurement takes from
178 10 s to 1 min depending on the system's properties.
179 The precision and accuracy of the DT-1200 are
180 described in the following sections.

2.1. Precision

181

Precision is a measure of the reproducibility. This section presents results concerning the precision of both the acoustic and the electroacoustic sensors.

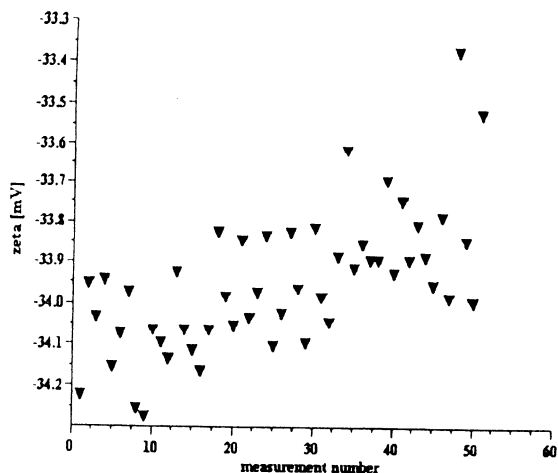
The attenuation spectra in Fig. 1 illustrate the precision of the acoustic sensor. These spectra were measured on alumina Sumitomo AA-2 and silica Ludox. The alumina sample was measured 10 times in a row, while the silica sample was measured 11 times in a row. Corresponding median particle sizes are given in Table 1. It is seen that absolute variation of the median particle size is 0.9% for alumina and 1.5% for silica. These numbers illustrate the precision of the acoustic sensor.

Figs. 2 and 3 illustrate the precision of the

5 Table 1
6 Median particle size

7 Alumina	2.015	2.076	2.057	2.092	2.065	2.047	2.035	2.075	2.039	2.085
8 Silica	0.03	0.029	0.029	0.029	0.029	0.03	0.03	0.029	0.03	0.03

1
2



16
20 Fig. 2. Multiple ζ -potential measurements of 10 wt.% silica
22 Ludox.

197 electroacoustic sensor. Fig. 2 shows the results of
198 51 continuous CVI measurements for silica Ludox.
199 It is seen that the precision of the absolute value
200 of the ζ -potential measurements is a fraction of a
201 mV. Fig. 3 shows titration curves for three identical
202 samples of 6 wt.% alumina with particles about

100 nm in size. It is seen that the precision in
determining the isoelectric point is about 0.1 of a
pH unit.

2.2. Accuracy

Accuracy characterizes the correlation between
real and measured values. The accuracy of PSD
measurement is a measure of the adequacy of the
measured particle-size distribution. In order to
determine the accuracy of PSD one needs a stan-
dard system with a known particle-size distribu-
tion. We used BCR silica quartz with a median
size of about 3 μm ; this is a PSD standard in
Germany.

Fig. 4 shows the standard particle-size distribu-
tion and that measured with the DT-1200. The
difference in median particle size between the stan-
dard and DT-1200 measurements is less than 1%.
At the same time there is some difference in the
amount of small particles. The results indicate that
the acoustic sensor determines the median size
with an accuracy of 1% and the standard deviation
with an accuracy of about 5%.

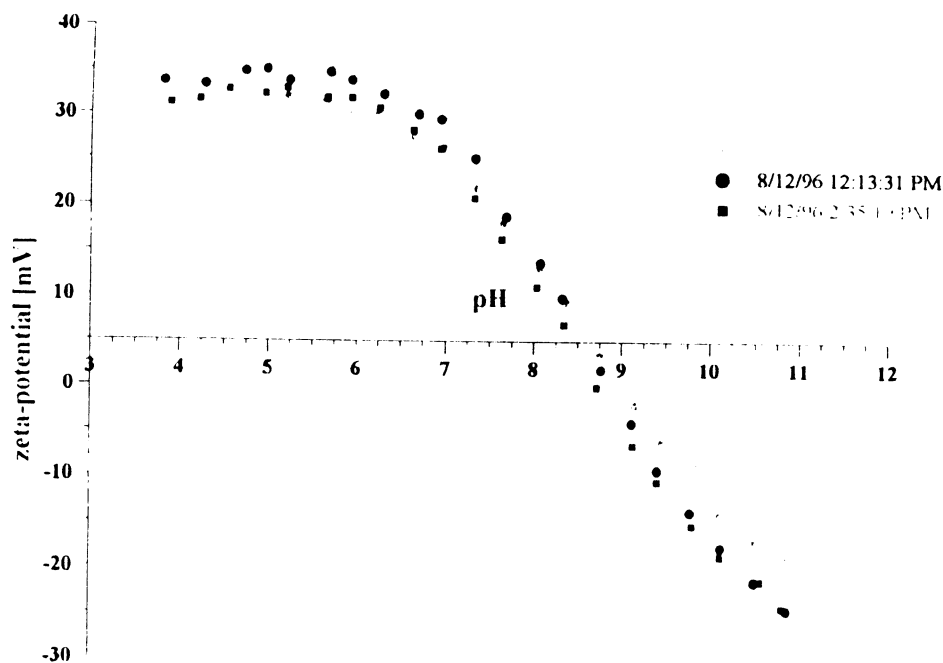
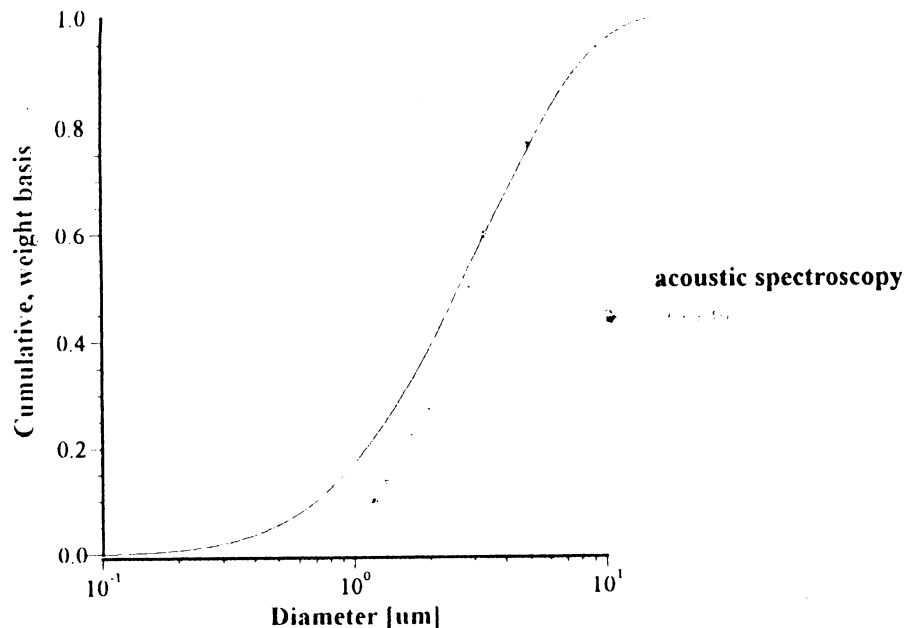


Fig. 3. Titration of three samples of the same 6 wt.% alumina.

26
30



38 Fig. 4. Particle-size distribution of the silica quartz BCR. The acoustic measurement was performed with 11 wt.% particles in ethanol. 39

225 Testing the accuracy of ζ -potential measure-
 226 ments is much more complicated because there is
 227 no ζ -potential standard for concentrated systems.
 228 The lack of an electroacoustic theory for concen-
 229 trated systems creates additional complexity. Our
 230 experience is that CVI makes it possible to measure
 231 ζ with the almost same accuracy as micro-
 232 lectrophoresis.

233 3. Titration experiment

234 3.1. Materials

235 Titration experiments have been performed with
 236 the two different materials: alumina and rutile. We
 237 chose these materials because of the different
 238 expected values of their isoelectric points. The
 239 isoelectric point of rutile is at about pH=4,
 240 whereas that for alumina is around pH=9.

241 A concentrated aqueous rutile slurry was
 242 obtained from E.I. Du Pont de Nemours. It is
 243 referred to commercially as R746 and is normally
 244 supplied at a weight content of 76.5% (44.5% by
 245 volume). The density of the particles was

4.06 g cm⁻³, which is slightly less than for regular 246
 rutile because of the various surface modifiers used 247
 to stabilize the slurry. A pH titration was per- 248
 formed with a relatively concentrated sample, 249
 7 vol.%. The sample was diluted with distilled 250
 water and adjusted to pH 8.5 with potassium 251
 hydroxide. The median particle size of this rutile 252
 slurry is about 0.3 μm according to the manufactur- 253
 er's data. 254

The alumina slurry was 11.6 wt.% or 4 vol.%; 255
 the initial pH was 4. This sample was used in 256
 titrations without additional dilution. The median 257
 particle size of the alumina particles was unknown. 258

259 3.2. Results and discussion

Electroacoustic measurements of ζ potential 260
 confirmed the expected values of isoelectric points 261
 for both alumina and rutile. Corresponding titra- 262
 tion curves are shown in Fig. 5. 263

According to general colloid chemical principles, 264
 dispersed systems lose stability at a pH close to 265
 the isoelectric point. Particle aggregation changes 266
 the particle-size distribution. This in turn will 267
 affect the attenuation spectra. The experiment 268

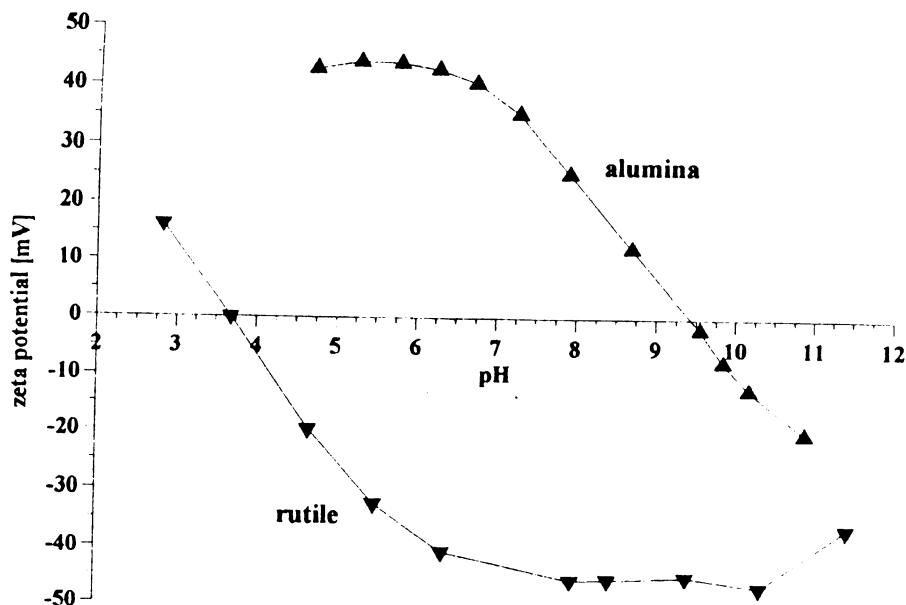
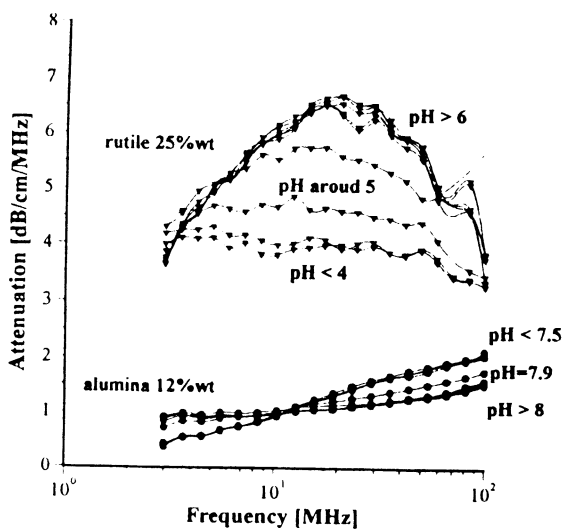


Fig. 5. Titration ζ -potential curves for 7 vol.% rutile and 4 vol.% alumina.

48
48

269 shows, indeed, that the attenuation spectra changes
270 with pH for both alumina and rutile (Fig. 6).

271 It is interesting that in both cases the attenuation
272 spectra remain unchanged up to a certain pH. In
273 the case of alumina it is stable up to $\text{pH} = 7.3$; in



52

57 Fig. 6. Attenuation spectra for 7 vol.% rutile and 4 vol.% alumina at different pH values.
58

the case of rutile, this critical pH is 5.9. The
274 attenuation spectra change beyond this critical pH. 275

This critical pH marks a range of aggregation
276 stability. Alumina is stable for pH below 7.3
277 whereas rutile is stable for pH above 5.9. In both
278 cases this critical pH corresponds to the same
279 value of ζ potential, about 30 mV. Both dispersed
280 systems lose their stability when the ζ potential
281 drops to the level of 30 mV. 282

A continuous change of pH beyond the critical
283 point causes a fast change of the attenuation
284 spectrum. It reaches another stable level in both
285 cases. The existence of this other, pH-independent
286 attenuation spectrum is a very interesting peculiar
287 feature that is common for both systems. 288

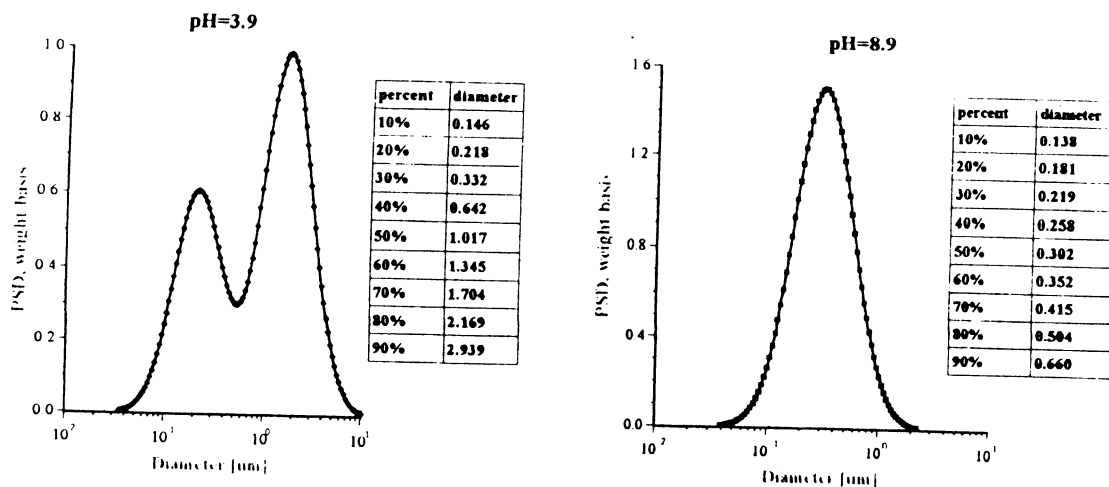
In the case of alumina, the attenuation spectrum
289 remains the same over a wide pH range from 8.2
290 to 11. The attenuation spectrum of rutile at pH
291 below at least 4 does not change either. This means
292 that, for some reason, particle-size distribution
293 does not change in the vicinity of the isoelectric
294 point. The systems are certainly unstable at these
295 pH values; however, there is a factor which pre-
296 vents particles from collapsing into large
297 aggregates. 298

299 Particle-size distributions are shown in Figs. 7
300 and 8 for various pH values. The error analysis
301 presented in the following section proves that the
302 distribution becomes bimodal beyond the critical
303 pH. However, the size of the aggregates does not
304 exceed several μm .

305 We believe that the bimodal particle-size distri-
306 butions are stable in time because of the stirring.
307 The titration experiment requires samples to be
308 stirred to achieve quick and homogeneous mixing

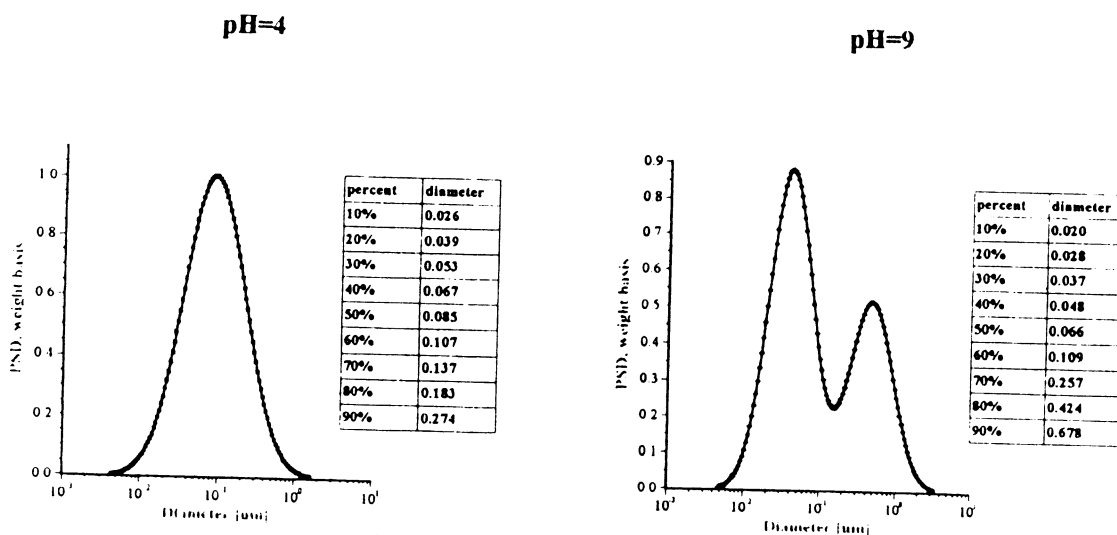
of the added chemicals. Shear stresses caused by 309
this stirring might break up large aggregates. This 310
shear can be a factor which restricts the size of the 311
aggregate. This idea can be tested experimentally 312
in the future by making measurements at different 313
stirring rates. 314

There is another unsolved question, however. 315
We do not know whether the aggregation observed 316
is reversible. Both systems used did not allow us 317
to reach the ζ potential above the critical value 318



63
68

Fig. 7. Particle-size distribution of stable and unstable 7 vol.% rutile.



72
78

Fig. 8. Particle-size distribution of stable and unstable 4 vol.% alumina.

1
2

319 (30 mV) after crossing the isoelectric point. The
320 ζ -potential value is restricted by increasing ionic
321 strength at high pH for the alumina and at low
322 pH for the rutile. We need another material with
323 an isoelectric point at the middle pH range in
324 order to answer this question.

325 3.3. Error analysis

326 When calculating PSD from the attenuation
327 spectra, the DT-1200 analysis program searches
328 for particle-size distributions with predefined
329 shape. The five different shapes are used: mono-
330 disperse, lognormal, bimodal, modified lognormal
331 [20] and modified bimodal. This approach makes
332 it possible to increase the number of adjustable
333 parameters in steps and also to implement a priori
334 information. The number of adjustable parameters
335 is equal to 1 for monodisperse PSD (size), 2 for
336 lognormal (size and standard deviation) and 4 for
337 bimodal (two mode sizes, standard deviation of
338 the mode assumed to be the same for both of them
339 and the relative weight of modes). Modified log-
340 normal and bimodal PSDs give an opportunity to
341 use a priori information about minimum and/or
342 maximum size.

343 The analysis software searches for the best
344 values of adjustable parameters by minimizing the
345 deviation between experimental and theoretical
346 attenuation spectra calculated for the various
347 PSDs. The result of this search is five best distribu-
348 tions (best monodisperse, best lognormal, best
349 bimodal, best modified lognormal and best modi-
350 fied bimodal).

351 There is a theoretical error corresponding to the
352 best fit achieved with a distribution of particular
353 shape. Comparison of these errors allows a deci-
354 sion to be made about which distribution is the
355 most suitable: the smaller error, the better the
356 PSD. The error value decreases with increasing
357 number of adjustable parameters. However, this
358 does not mean that a bimodal distribution is
359 always better than a lognormal one because the
360 reliability of the PSD is reciprocally proportional
361 to the number of adjustable parameters. Although
362 an increase in the number of adjustable parameters
363 improves the theoretical fit, it reduces reliability.

364 It is obvious that there is some optimum number

of adjustable parameters. Experimental error 365
should be used in order to define this optimum 366
number. According to Ocaam's principle, we 367
should stop adding adjustable parameters when 368
the theoretical error becomes smaller than the 369
experimental error. 370

The values of theoretical and experimental errors 371
are shown on Fig. 9 for both alumina and rutile. 372
Errors of the lognormal and bimodal distributions 373
are almost identical for pH values corresponding 374
to the stable systems: >5.9 for rutile and <7.3 375
for alumina. The larger number of adjustable 376
parameters for the bimodal PSD causes no 377
improvements in theoretical fit. This means that 378
there is no reason to claim a bimodal PSD for 379
 $\text{pH} > 5.9$ for rutile and $\text{pH} < 7.3$ for alumina. 380

The error of the theoretical fit for the lognormal 381
distribution becomes much larger than that for the 382
bimodal one at $\text{pH} < 5.9$ for rutile and $\text{pH} > 7.3$ 383
for alumina. A lognormal distribution fails to fit 384
experimental attenuation spectra in this pH range. 385
The much smaller theoretical error is the reason 386
to claim a bimodal PSD for these two pH points. 387

This error analysis yields the conclusion that a 388
lognormal distribution is not suitable for charac- 389
terizing unstable dispersed systems. This type of 390
particle-size distribution does not reflect ade- 391
quately the formation of aggregates. 392

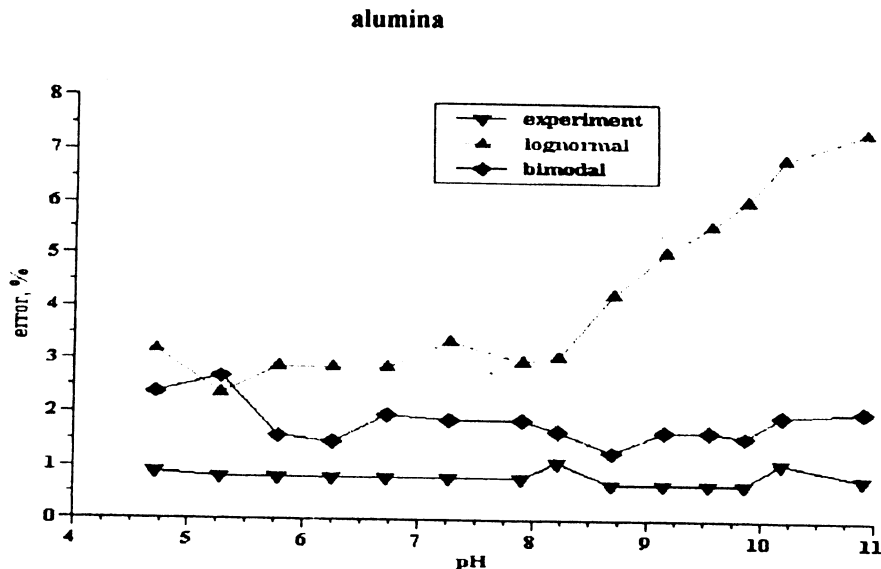
4. Conclusions 393

394 Combined acoustic and electroacoustic spectro-
scopy provides independent characterization of 395
particle-size distribution (PSD) and ζ potential. In 396
essence, the acoustic spectra provide PSD informa- 397
tion, whereas the electroacoustic signal (colloid 398
vibration current, CVI) yields ζ potential. 399

Acoustic spectroscopy can characterize the 400
median particle size with a precision and accuracy 401
of about 1%. The width of the distribution can be 402
characterized with a precision of about 1% and an 403
accuracy of about 5%. 404

Values of ζ potential can be determined with a 405
precision of a fraction of a mV and an accuracy 406
about several mV, depending on the particle 407
volume fraction. 408

Acoustic attenuation spectra and CVI measufed 409



rutile

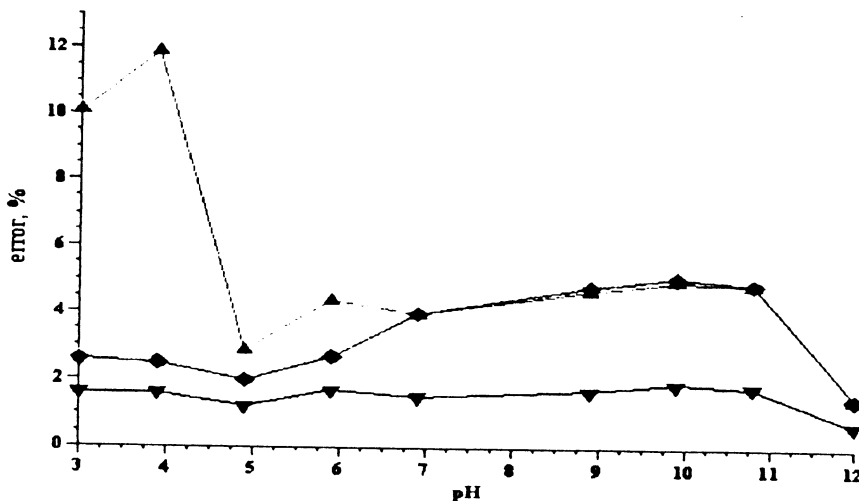


Fig. 9. Errors of theoretical fit achieved with lognormal and bimodal distributions for different pH values.

80
86

410 for concentrated 7 vol.% rutile and 4 vol.% alu-
411 mina dispersions show pronounced changes caused
412 by pH. These changes are associated with aggrega-
413 tive stability. Both dispersions lose stability within
414 ± 2 pH units of the isoelectric point. Both disper-

sions become unstable when the absolute value of
ζ potential drops below 30 mV.

The particle-size distribution for both disper-
sions becomes bimodal near the isoelectric point.
This bimodal distribution remains quite stable

1
2

420 within ± 2 pH units in the vicinity of the isoelec-
421 tric point.

422 A lognormal PSD is not very suitable for charac-
423 terizing such unstable systems. The fitting error
424 between the experimental spectra and the lognor-
425 mal PSD is much larger than the error for a
426 bimodal PSD. The lognormal PSD fails to reflect
427 properly the formation of aggregates.

428 References

- 429 [1] P.S. Epstein, R.R. Carhart, The absorption of sound in
430 suspensions and emulsions, *J. Acoust. Soc. Am.* 25 (3)
431 (1953) 553–565.
- 432 [2] J.R. Allegra, S.A. Hawley, Attenuation of sound in suspen-
433 sions and emulsions: theory and experiments, *J. Acoust.*
434 *Soc. Am.* 51 (5) (1972) 1545–1564.
- 435 [3] A.S. Dukhin, P.J. Goetz, Acoustic spectroscopy for con-
436 centrated polydisperse colloids with high density contrast,
437 *Langmuir* 12 (21) (1996) 4987–4997.
- 438 [4] A.S. Dukhin, P.J. Goetz, C.W. Hamlet, Acoustic spectro-
439 scopy for concentrated polydisperse colloids with low den-
440 sity contrast, *Langmuir* 12 (21) (1996) 4998–5004.
- 441 [5] D.J. McClements, Ultrasonic characterization of emul-
442 sions and suspensions, *Adv. Colloid Interface Sci.* 37
443 (1991) 33–72.
- 444 [6] B.J. Marlow, D. Fairhurst, H.P. Pendse, Colloid vibration
445 potential and the electrokinetic characterization of concen-
446 trated colloids, *Langmuir* 4 (3) (1983) 611–626.
- 447 [7] F. Booth, J. Enderby, On electrical effects due to sound
448 waves in colloidal suspensions, *Proc. Am. Phys. Soc.* 208A
449 (1952) 32.
- 450 [8] R.W. O'Brien, W.N. Rowlands, R.J. Hunter, Determining
charge and size with the acoustosizer, in: National Institute
of Standards and Technology Special Publication 856, 451
USA Department of Commerce, 1993, pp. 1–22. 452
- [9] R.W. O'Brien, Electro-acoustic effects in a dilute suspen- 454
sion of spherical particles, *J. Fluid Mech.* 190 (1988) 455
71–86. 456
- [10] A.S. Dukhin, P.J. Goetz, Acoustic and electroacoustic 457
spectroscopy, *Langmuir* 12 (19) (1996) 4334–4344. 458
- [11] A.H. Harker, J.A.G. Temple, Velocity and attenuation of 459
ultrasound in suspensions of particles in fluids, *J. Phys.*
D.: *Appl. Phys.* 21 (1988) 1576–1588. 460
- [12] A.H. Harker, P. Schofield, B.P. Stimpson, R.G. Taylor, 461
J.A.G. Temple, Ultrasonic propagation in slurries,
Ultrasonics 29 (1991) 427–439. 462
- [13] R.L. Gibson, M.N. Toksoz, Viscous attenuation of acous- 463
tic waves in suspensions, *J. Acoust. Soc. Am.* 85 (1989) 464
1925–1934. 465
- [14] H.P. Pendse, T.A. Strout, A. Shanna, Theoretical consider- 466
ation in acoustophoretic analysis of concentrated colloids,
in: National Institute of Standards and Technology Special 467
Publication 856, USA Department of Commerce, 1993, 468
pp. 23–39. 469
- [15] T.A. Strout, Attenuation of sound in high-concentration 470
suspensions: development and application of an oscillatory
cell model, Thesis, The University of Maine, 1991. 471
- [16] S.S. Dukhin, B.V. Derjaguin, in: E. Matijevic (Ed.), 472
Electrokinetic Phenomena in Surface and Colloid Science,
vol. 7, Wiley, New York, 1974. 473
- [17] T.A. Vorobyeva, I.N. Vlodayets, S.S. Dukhin, *Colloid. J.* 474
USSR 32 (1970) 189. 475
- [18] P.F. Rider, R.W. O'Brien, The dynamic mobility of par- 476
ticles in a non-dilute suspension, *J. Fluid. Mech.* 257 477
(1993) 607–636. 478
- [19] P.F. Rider, Sound wave mobilities in a nondilute suspen- 479
sion of spheres, *J. Colloid Interface Sci.* 172 (1995) 1–13. 480
- [20] R.R. Irani, C.F. Callis, *Particle Size: Measurement, 481
Interpretation and Application*, Wiley, New York, 1971. 482